13th International Conference on
Structural Health Monitoring of Intelligent Infrastructure
DOI: 10.3217/978-3-99161-057-1-017

Evolving reliability-based condition indicators for structural health monitoring into a digital twin of a cable-stayed bridge

Martin Herbrand[1, ORCID 0000-0003-2513-2686], Marc Wenner[2], Alex Lazoglu[3], Christof Ullerich[4], Gerhard Zehetmaier[1], Steffen Marx[2]
[1]WTM Engineers GmbH, Johannisbollwerk 6-8, 20459 Hamburg, Germany
[2]MKP GmbH, Zum Hospitalgraben 2, 99425 Weimar, Germany
[3]DB InfraGO AG, Zum Güterbahnhof 9, 99085 Erfurt, Germany
[4]Hamburg Port Authority AöR, Neuer Wandrahm 4, 20457 Hamburg
email: m.herbrand@wtm-hh.de, marc.wenner@marxkrontal.com, alex.lazoglu@al-ing.com,
christof.ullerich@hpa.hamburg.de, g.zehetmaier@wtm-hh.de, steffen.marx1@tu-dresden.de

ABSTRACT: In Germany, the bad condition of many older bridges and changes in the code provisions often result in deficits after assessment and recalculation. In case the necessary structural safety is not provided, structural health monitoring can be employed to gain knowledge about the time variant actions, the progression of structural damage and the overall condition of structures. To allow for effective use of the usually dense monitoring raw data, the derivation of condition indicators is key, since they indicate a need for action for the owners and the engineers. At the same time, real-time data as well as comprehensive condition indicators are key elements for creating a Digital Twin of a structure, as a Digital Twin requires a bidirectional flow of data, which affects the physical entity of the twin. In this paper, a method for deriving condition indicators from monitoring data is described which was developed for a large cable-stayed bridge, the Köhlbrand Bridge in Hamburg, Germany. The method allows for the calculation of a reliability index as a time variant condition indicator based on dynamic monitoring data, which is then implemented into a Digital Twin of the structure.

KEY WORDS: SHM, reliability, condition indicators, condition monitoring, digital twin, bridges.

1 INTRODUCTION

Due to the poor condition of many older bridges and changes in the regulations, there are often deficits in the recalculation of existing bridges according to the German recalculation guidelines (NRR) [1]. If the required structural safety cannot be verified using standardized load models and modified resistance models in accordance with the various NRR standards, structural measurements can be carried out for a limited period or as continuous structural health monitoring (SHM) to gain knowledge about actions that vary over time. This makes it possible, for example, to derive object-specific traffic load models by using complex algorithms and models to infer the traffic volume and traffic composition based on structural measurements [2]-[4]. In the case of time variant physical state variables, an approach can be to reduce these to extreme values in defined time intervals and describing the frequency of their occurrence using approximation functions [5],[6]. These approximation functions allow for a prediction of which extreme values of the state variable will occur in the future [7] and what reliability against structural failure will result from this [8]. It is important here that sufficiently long measurement periods are available for such an investigation [9] and that the long-term stability of the measurement system is guaranteed for the measurement period [10].

The general aim of SHM is to assess the condition or performance of the structure. The key to this is the derivation of condition indicators for the structure which can relate, for example, to the state of preservation, safety or maintenance [11] and indicate to operators and engineers any need for action. Key figures relating to structural safety can be determined using a component-based or system-based approach [12]. In the simplest case, for example, a physical state variable of an individual component is compared with a corresponding threshold value to determine a degree of utilization. However, since these utilization rates are based on different actions, materials and failure modes with different variability, a utilization rate does not allow any conclusions to be drawn about the existing risk and, strictly speaking, only enables a binary assessment of the risk (exceedance or no exceedance). In this article, a procedure is therefore explained and implemented using the example of the Köhlbrand Bridge in Hamburg, which allows a reliability index to be derived from the dynamic monitoring ring data as a time-varying condition indicator in relation to a buckling monitoring. As part of the smartBRIDGE Hamburg project, the condition indicator was integrated into a digital twin of the structure, which contains a total of over 40 different condition indicators.

Figure 1. Köhlbrand Bridge Hamburg (source: HPA-archive Martin Elsen).

Since the buckling verification in this example is to be classified as a decisive structural check, this safety index does not refer to the system reliability but is determined for the

DOI: 10.3217/978-3-99161-057-1-017

critical components of the structure. The structure and the problem are explained in more detail in the following chapter.

2 PROBLEM DESCRIPTION AND MEASUREMENT MEASURES

2.1 Problem Description

As one of Hamburg's most important traffic arteries, the Köhlbrand Bridge has been crossing the Köhlbrand between the Elbe island of Wilhelmsburg and Waltershof since 1974. The middle section, the river bridge, is a two-legged cable-stayed bridge with individual spans of 97.5 m, 325 m and 97.5 m (Fig. 1). The superstructure is designed as a single-cell steel box girder with an orthotropic deck [13].

In the course of a recalculation of the current bridge carried out in 2016 in accordance with levels 1 and 3 of the German recalculation guideline [1], the verification against buckling of the web and base plates in the pylon area for the required target load level (i. e. LM1 according to the German bridge code DIN-FB 101) could not be provided [14],[15]. The buckling verifications were carried out using the so-called reduced stress method in accordance with the German code for steel bridges DIN-FB 103 [16]. Due to the normal force distribution in the stiffening girder, the pylon area represents the decisive area for the buckling checks, with the checks being exceeded by up to 30 %. As part of level 3 of the recalculation guideline [17], cable force measurements were carried out to determine the stresses from permanent actions, which resulted in slightly lower longitudinal compressive stresses. However, the buckling check could not be provided here either using the reduced stress method. The degrees of utilization resulting from the calculation according to level 3 are shown in Fig. 2.

The iterative verification using the method of effective widths according to DIN FB 103 [16] Chapter III-4 also led to an intolerable exceedance. As a result, a distance requirement of 50 m for trucks was added to the existing truck overtaking ban as a compensatory measure in accordance with the 1st amendment to the recalculation guideline [17] in order to reduce the traffic loads on the outer lanes and to be able to apply the reduced BK60 load model in accordance with the older traffic load code DIN 1072 (1967) [18]. However, this measure leads to considerable disturbance of regional and national traffic in Hamburg.

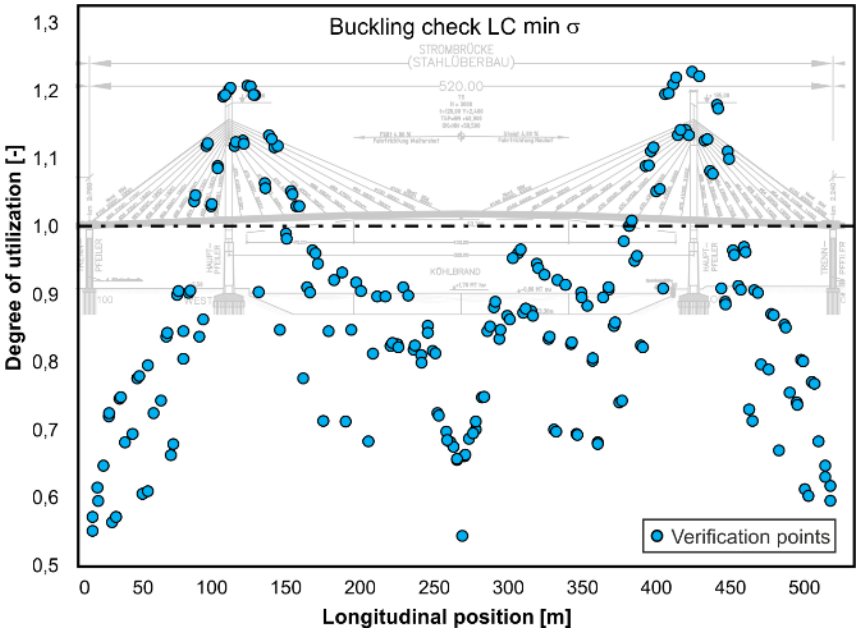

Figure 2. Utilization of buckling verification after recalculation level 3 (taken from [15])

To be able to lift the distance requirement in the medium term, early monitoring measures were commissioned by the Hamburg Port Authority AöR (HPA) as part of the smartBRIDGE Hamburg project [19], the piloting of a digital twin of the Köhlbrand Bridge. These include strain measurements in the web and floor plates in the area at risk of buckling, as well as acceleration measurements on some of the harp cables to assess the risk of buckling. To assess the risk of buckling, the long-term buckling monitoring data from a 12-month period from July 2019 to June 2020 was evaluated as a first step. The data evaluation has recently been extended to December 2024. The aim of the monitoring is to determine whether there is a risk of buckling for the superstructure in the current load situation with the distance requirement and whether there are sufficient load-bearing reserves to lift the distance requirement. Probabilistic evaluation concepts of different levels of complexity were developed for this purpose. In the following, a simplified evaluation concept for the detection of buckling risk is described and applied to the long-term data of the buckling monitoring to derive a suitable condition indicator for assessing the risk of buckling.

2.2 SHM Measures

As the buckling of the web and floor plates could not be verified analytically, even with the aid of cable force measurements, MKP GmbH and WTM Engineers GmbH developed a measurement concept for a continuous structural monitoring. Variable actions in the superstructure were to be recorded via strain measurements on the superstructure and converted into acting stresses. In addition to the strain measurements, sensors for measuring the temperature of the structure, meteorological data (air temperature, radiation, humidity, wind direction and wind speed) and accelerations on the superstructure were provided. In conjunction with a Weigh-in-motion system installed on the structure, the additional sensors record the external effects on the bridge structure almost completely and should, for example, make it possible to assign the measured stress components in the web and floor plates to the different traffic load components. In addition, acceleration sensors (y- and z-axis) were permanently installed on 22 harp cables, which corresponds to a quarter of all cables on the current bridge. These sensors enable, among other things, the continuous determination of the cable forces,

DOI: 10.3217/978-3-99161-057-1-017

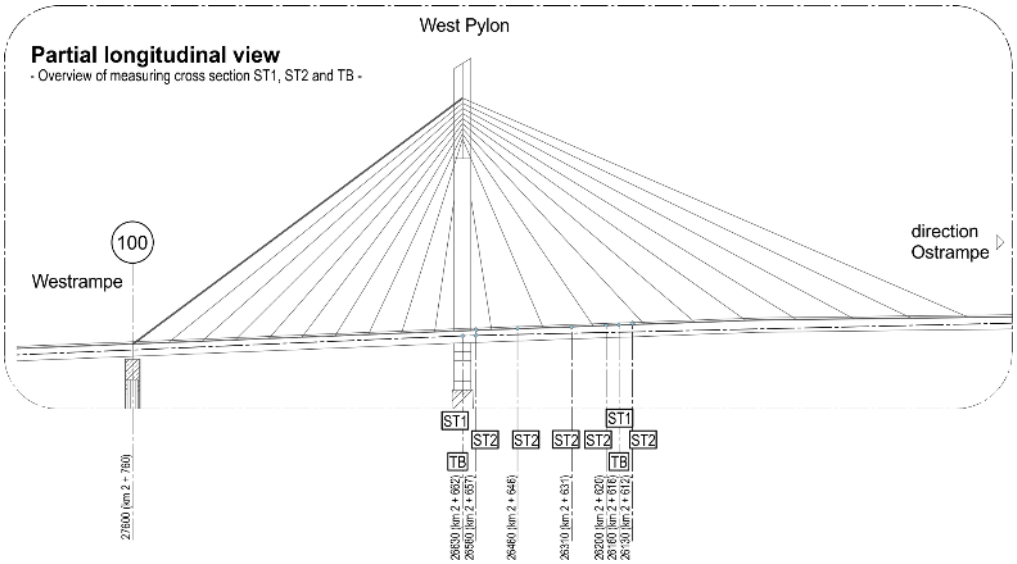

Figure 3. Position of the measuring cross-sections in longitudinal direction (source: MKP GmbH)

on which the stresses due to dead load of the superstructure depend on to a large extent.

The strain measurements were carried out in a total of seven measurement cross-sections along the longitudinal axis of the current bridge (Fig. 3).

A distinction is made between two types of measuring cross-section: Measuring cross-section ST1 (Fig. 4a) comprises nine Y-rosette strain gauges (arrangement of the measuring elements 0°/45°/90°) on the web, bottom and top plates, through which three independent directions of strain are recorded to determine the main stress states. Measuring cross-section ST2 (Fig. 4b) is a reduced measuring cross-section and comprises four T-rosette type sensors in the corners of the box girder. These record two directions of strain (arrangement of the measuring grids 0°/90°) to accurately determine the strain distribution in the horizontal and vertical directions, considering transverse strain influences, but without the possibility of determining the main stress directions. The details of the strain sensor arrangement of the ST1 and ST2 measuring cross-sections are shown in Figures 4c and 4d. The strain sensors of the monitoring system measure at a frequency of 100 Hz, whereby the minimum (min), maximum (max) and average values (avg) of the strains and stresses of 5-minute intervals are stored and evaluated.

The sensor system is very extensive with a total of 94 strain sensors in the superstructure, 44 acceleration sensors on the cables, nine acceleration sensors on the superstructure, 20 temperature sensors and eight additional meteorological sensors. The scope of the measurements can also be explained by the continued use of the measuring system as part of the smartBRIDGE Hamburg project [19], in which additional condition indicators were developed and monitored. In addition, the aim was to check whether the Finite Element (FE) hybrid model of the structure provides accurate strain states under a defined load, which requires an accurate measurement of the strain distribution over the entire cross-section height.

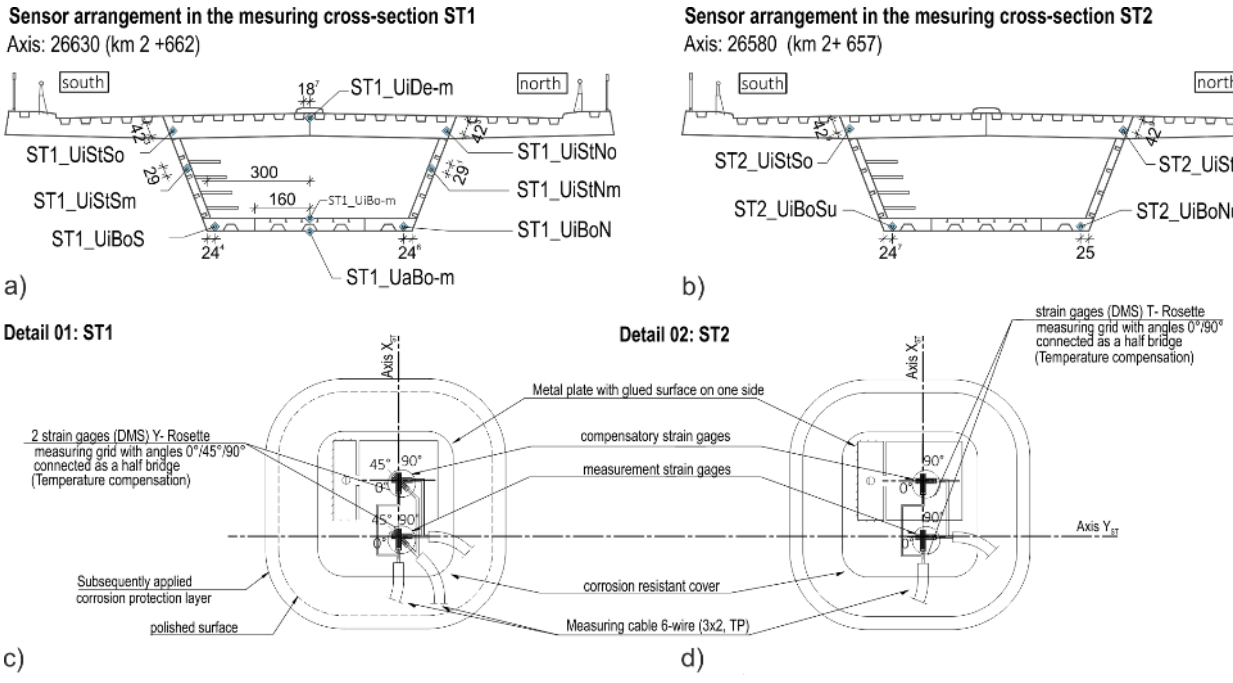

Figure 4. Measuring cross-sections and arrangement of the strain sensors (Source: MKP GmbH)

DOI: 10.3217/978-3-99161-057-1-017

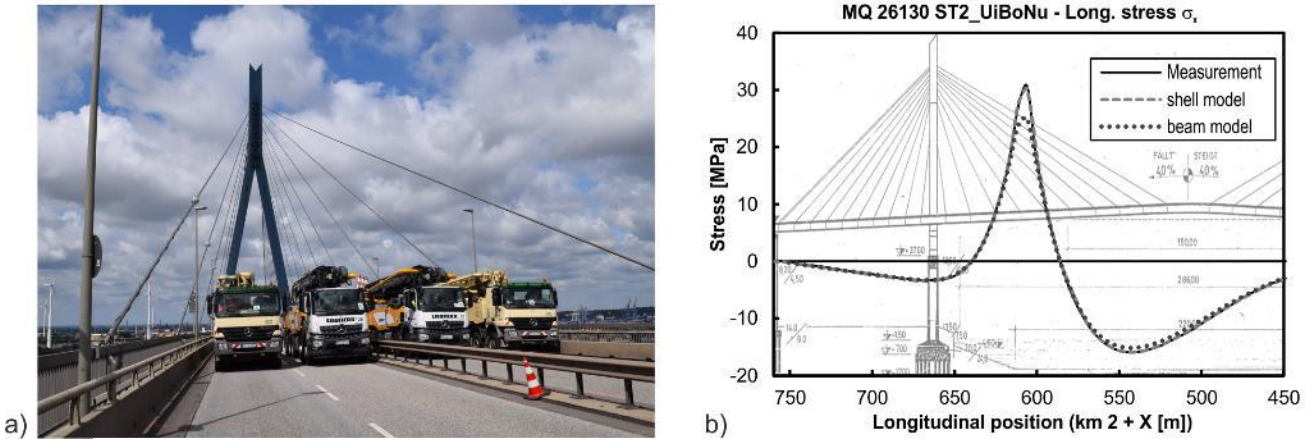

Figure 5. a) Load test on the structure; b) Comparison of measured and calculated longitudinal stresses (source: WTM Engineers)

2.3 Load Tests

Defined load tests and model calibrations are required to verify the plausibility of the stress values measured on the structure and to be able to relate them to the stress values calculated using normative load models. For this reason, the sensor system installed in June 2019 was tested as part of extensive load tests during a full closure of the structure in July 2019. The structure was driven over with four concrete pump vehicles with a total weight of around 180 tons in different formations (Fig. 5a). In addition, measurements were carried out on cables under ambient and harmonic excitation with installed and removed dampers to determine the damping parameters. The evaluation of the load tests generally showed very good agreement between the measured longitudinal stresses and the stresses of the FE models [20]. The influence line of a real crossing and the influence line of an FE beam and shell model are compared as an example in Fig. 5b. The FE shell model shows almost complete agreement with the measured longitudinal stresses, while the beam model slightly underestimates the stresses. This is to be expected as longitudinal stress concentrates in the corner areas of the box girder, an effect which is not captured by a beam model. The functionality and accuracy of the monitoring system could thus be confirmed by the field test and the FE model.

3 EVALUATION METHODOLOGY

3.1 Semi-probabilistic evaluation concept

The developed concept for the monitoring-based buckling analysis is shown in Fig. 6. The concept is focused on the metrological determination of the acting stresses, whereby the resistance side of the buckling analysis is not directly included in the consideration (Section 3.2). The following two methods are available as examples for determining the design stresses from variable effects: Direct measurement of the steel stresses in the buckling field (method (a)) and indirect measurement by determining the external actions (method (b)).

Direct measurement according to method (a) requires strain measurement on the cross-section using strain gages at the relevant points. The existing stresses from dead loads can be determined by cable force measurements or taken from the recalculation. The extreme values of stresses from a relatively short measurement period (e.g. one year) can be converted into design values of the acting stresses by a statistical evaluation of the variable stresses. On the resistance side, the permissible stresses according to DIN FB 103 [16] are applied. The target values for reliability can be taken from EC0 [21].

In the indirect measurement according to method (b), the main effects on the current bridge are recorded and characteristic values for the respective actions are derived. These can in turn be applied to the structural FE model to determine the characteristic stresses in the buckling areas. The design value of the compressive stress can then be determined conventionally using the design partial safety factors and combination coefficients of German bridge codes. Alternatively, the combination coefficients can be derived individually based on the data from the long-term monitoring.

In this article, the design stresses are determined based on method (a), as this method does not require a distinction between different types of action, but only a distribution function for the measured extreme values is derived.

3.2 Determination of target reliability

The total design resistance stresses in the ultimate limit state (ULS) are determined in accordance with the recalculation of the bridge [14],[15] based on the concept of reduced stresses in accordance with DIN-FB 103. The design resistance of the variable compressive stresses in the longitudinal direction $\sigma_{Q,Rd}$ results from the difference of the total design resistance according to DIN FB 103 $\sigma_{Rd,DIN\text{-}FB}$ minus the design value of the permanent actions $\sigma_{g,Ed}$. For the area of the base plate, the design resistance of the variable compressive stresses results according to Eq. (1).

$$\sigma_{Q,Rd} = \sigma_{Rd,DIN-FB} - \sigma_{g,Ed} = -113\ N/mm^2 \qquad (1)$$

DOI: 10.3217/978-3-99161-057-1-017

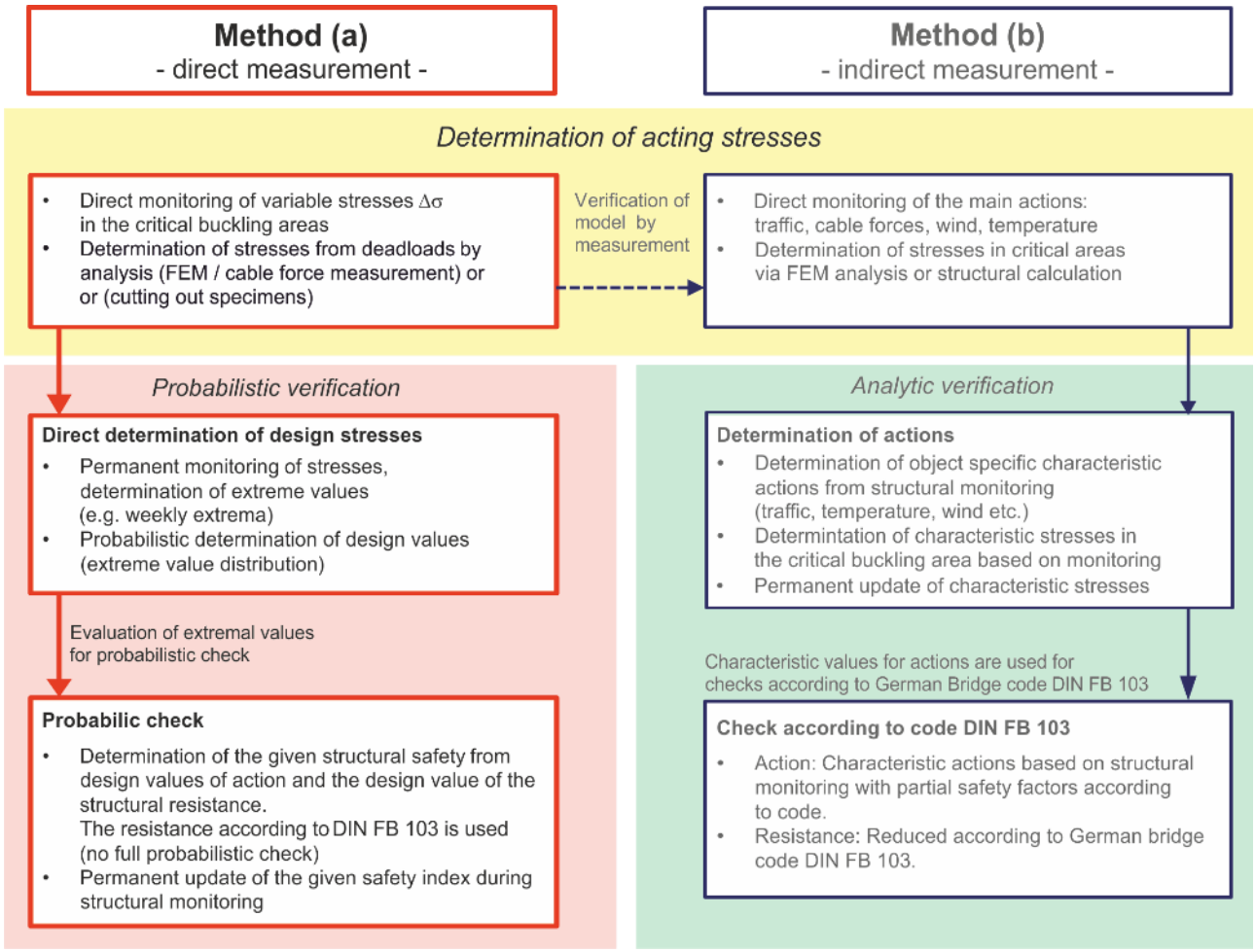

Figure 6. Concept for compensating for safety deficits through SHM (source: WTM Engineers)

For the area of the web plates, the design resistance of the variable compressive stresses at the point of intersection with the base plate are given by Eq. (2).

$$\sigma_{Q,Rd} = \sigma_{Rd,DIN-FB} - \sigma_{g,Ed} = -123\ N/mm^2 \qquad (2)$$

Since the resistance side is not considered further when determining the design values of the action or when calculating the existing reliability, the target value of the reliability index for the actions E_d is determined with $\beta_E = \alpha_E \cdot \beta$ (EC0 [21], Eq. C.6a), with α_E = -0.7 and β = 3.8 according to EC0, Table C.2 [21].

For the case of normally distributed basic variables of the actions, Eq. (3) applies to the determination of the measurement value E_d.

$$E_d = m_E + \alpha_E \cdot \beta \cdot \sigma_E \qquad (3)$$

Here, m_E is the mean value of the actions with the standard deviation σ_E. The target value of the reliability index β thus refers to both permanent and variable loads. However, the evaluation concept presented here is based on the stresses from dead loads determined in the recalculation and only the design value of the variable stress is determined probabilistically from monitoring data. For this purpose, it should first be checked under which boundary conditions a separate consideration of permanent and variable actions is on the safe side. Permanent and variable loads can be divided on the safe side according to Eq. (4).

$$\begin{aligned} E_{g,d} + E_{Q,d} &= m_g + m_Q + \alpha_E \beta \sqrt{\sigma_g^2 + \sigma_Q^2} \\ &< m_g + m_Q + \alpha_E \cdot \beta (\sigma_g + \sigma_Q) \end{aligned} \qquad (4)$$

Due to the fact that the permanent actions are determined with $E_{g,d} = \gamma_g \cdot m_g$ and γ_g = 1.35, Eq. (4) can be transformed into Eq. (5).

$$\begin{aligned} E_{Q,d} &< m_g \left[\alpha_E \cdot \beta \cdot \frac{\sigma_g}{m_g} + 1{,}0 - \gamma_g \right] \\ &+ \left[m_Q + \alpha_E \cdot \beta \cdot \sigma_Q \right] \\ &< m_Q + \alpha_E \cdot \beta \cdot \sigma_Q \end{aligned} \qquad (5)$$

The estimate at the end of Eq. (5) is valid for the conditions $V_g = \sigma_g/m_g < 0.132$, γ_g = 1.35 and $\beta_E = \alpha_E \cdot \beta$ = 2.66. In the event that the aforementioned boundary conditions apply, the design value of the variable actions $E_{Q,d}$ can therefore be determined on the safe side with the target safety index $\beta_E = \alpha_E \cdot \beta$. These are generally complied with for normal bridge structures, as the coefficient of variation V_g for dead loads should be well below 10 %. As a cable-stayed bridge is a structure with a complex interaction between cable forces and stiffening girders, further investigations were carried out as part of the buckling monitoring to determine the variability of the self-weight stresses using Monte Carlo simulations. The previous consideration still only applies to the case of normally

DOI: 10.3217/978-3-99161-057-1-017

distributed variables, whereas the measured minimum values of the stresses are to be described here by an extreme value distribution of type I (Gumbel-distrubution). However, as this provides values that are on the safe side compared to a normal distribution, the design value of the variable actions $E_{Q,d}$ with the target safety index $\beta_E = \alpha_E \cdot \beta$ is determined on the basis of an extreme value distribution in the simplified procedure presented here.

3.3 Determining the rated values from measurement data

To determine the parameters of the extreme value distribution, the selected reference period must be chosen in such a way that the structure experiences a load series that recurs as evenly as possible during this period. In the case of an hourly evaluation, strong stress differences arise between day and night hours, as well as in the case of a daily evaluation between working days and weekends. This results in unfavorable standard deviations of the extreme values. A comparatively uniform exposure is obtained if a weekly evaluation is selected as the reference period [4],[22].

For a continuous monitoring period of one year, 52 weekly extreme values are available for determining the parameters of the distribution function. The standard deviation σ_x and the mean value m_x can be estimated from the available weekly extreme values, e.g. using the method of moments or the maximum likelihood method. The density and distribution function of the extreme value distribution type I (Gumbel distribution) for minimal values are given in Eqs. (6) and (7) [23].

Density function for minimum values:

$$f(x) = a \cdot \exp[a(x-u) - exp[a(x-u)]] \tag{6}$$

Distribution function for minimum values:

$$F(x) = 1 - \exp[-exp[a(x-u)]] \tag{7}$$

Using eqs. (8), (9) the parameters a and u of the distribution function can be determined.

$$a = \frac{\pi}{\sigma_x \cdot \sqrt{6}} \tag{8}$$

$$u = m_x + \frac{0{,}577216}{a} \tag{9}$$

A special characteristic of the extreme value distribution type I is that the standard deviation of the distribution function does not change when the reference period is altered. Accordingly, the extreme value distribution for a selected reference period results from the shift of the extreme value distribution along the horizontal axis by converting the expected values (Fig. 7). The initial reference period of one week can thus be adapted to the corresponding target period for the measurement.

The reference period can be converted by calculating the corresponding fractile value. The associated exceedance probability q is calculated for maximum values according to Eq. (10) [24].

$$q = 1 - \frac{1}{n_a \cdot a} \tag{10}$$

where
n_a values per year depending on the reference period of the extreme values (here $n_a = 52$)
a Return period or assessment period in years

Next, Eq. (10) must be adjusted for minimum values according to Eq. (11):

$$q = \frac{1}{n_a \cdot a} \tag{11}$$

The calculation of fractile values of an extreme value distribution type I is carried out for minimum values according to Eq. (12).

$$F^{-1}(x) = u + \frac{1}{a}\ln(-ln[1-q]) \tag{12}$$

where
q undercut probability

The characteristic value of the effect E_k for a reference period of 50 years is obtained as a 2% fractile value of the expected value of the annual extreme value distribution (with $q = 1/(1 \cdot 50) = 0.02$) or as a 0.038% fractile value of the expected value of the weekly extreme value distribution (with $q = 1/(52 \cdot 50) = 3.8 \cdot 10^{-4}$). The reference period for which the characteristic value of the action is to be determined cannot be clearly determined. While according to EC1 [25] the characteristic values for some types of action refer to a reference period of 50 years (e.g. wind or temperature), a return period of 1000 years is specified for the LM1 load model according to EC1-2. In [26] examples are given according to which reference periods between 50 and 1000 years were applied for characteristic traffic loads. Since no normative partial safety factor for variable loads is applied in the present evaluation, the choice of the reference period is of secondary importance, since the target value of the reliability for different reference periods according to EC0 [21], Eq. C.3 is to be

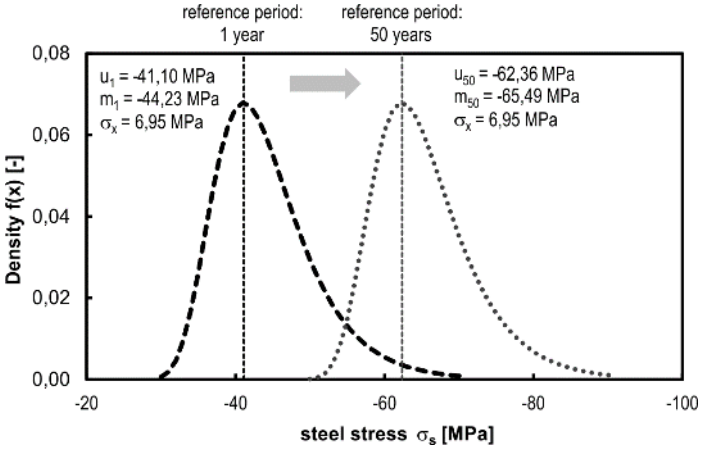

Figure 7. Exemplary conversion of the extreme value distributions for two reference periods (source: WTM Engineers)

DOI: 10.3217/978-3-99161-057-1-017

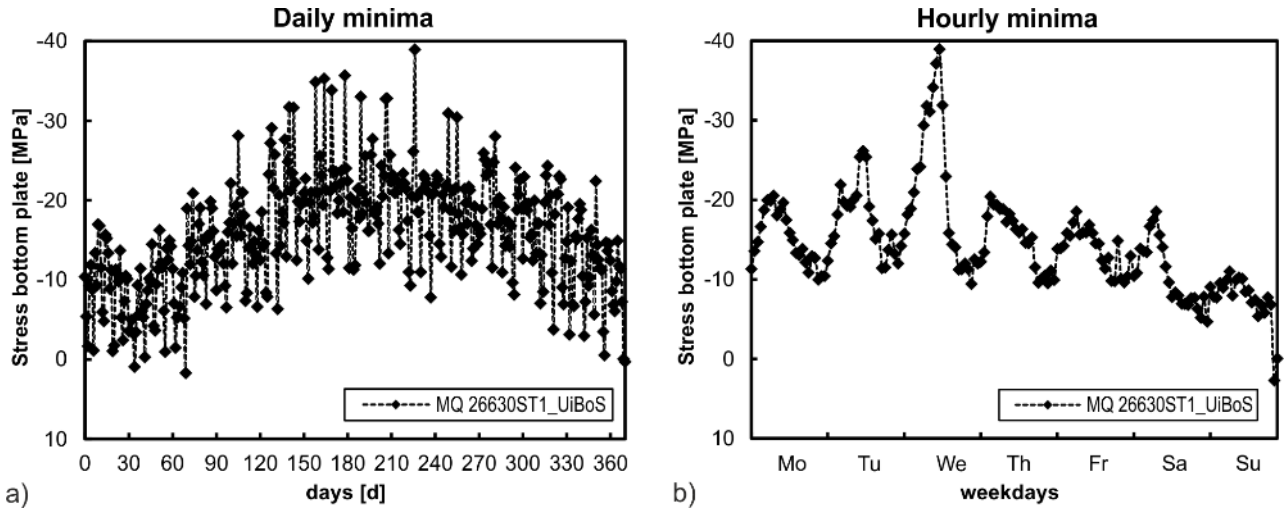

Figure 8. a) Daily minima of the measurement period; b) Hourly minima of a week in February 2020 (source: WTM Engineers)

converted in such a way that the same design values result for all reference periods.

It is important to note here that the weighting factors specified in the standards $\alpha_R = 0.8$ and $\alpha_E = -0.7$ only apply to a reference period of 50 years and may therefore only be applied to the value β_{50} (see also DIN 1055-100 [27], Eq. B.7).

The β_{50} index can be converted to other reference periods by applying the weighting factors for maximum values according to Eq. (13) (corresponding to EC0, Eq. C.3).

$$\Phi(\beta_n) = [\Phi(\beta_1)]^n = [\Phi(\beta_{50})]^{n/50} \quad (13)$$

Here, $\Phi(\beta)$ is the cumulative distribution function of the standardized normal distribution. Eq. (14) applies for minimum values with $\beta < 0$.

$$\begin{aligned}\Phi(\beta_n) &= 1 - [1 - \Phi(\beta_1)]^n \\ &= 1 - [1 - \Phi(\beta_{50})]^{n/50}\end{aligned} \quad (14)$$

To determine the design value of the action E_d, the fractile value of the action associated with the reference period n must be determined with the undercut probability $q = \Phi(\beta_{E,n})$ based on the characteristic value E_k determined according to Eq. (12).

The safety index for actions $\beta_{E,50}$ is 2.66 for a reference period of 50 years, which corresponds to an undercut probability of $q = \Phi(-2.66) = 0.4\%$.

4 VERIFICATION OF BUCKLING RISK

4.1 Evaluation of long-term data

The statistical evaluation of the variable stresses from the long-term monitoring is only shown here for the critical base plate of the measurement cross-section 26630 in the pylon area (see Fig. 3). The daily minima measured on the south side of the base plate during the measurement period are shown in Fig. 8a. The seasonal influence of the compressive stresses, which increase towards winter, can be clearly seen. The diurnal influences of temperature and traffic can also be seen in the hourly minima of a February week shown in Fig. 8b.

Figures 9a and 9b show the weekly minima of two measuring points each in the base plate and in the web in measuring cross-section 26630 over the measuring period. In addition to a greater variance, the measured values of the base plate on the

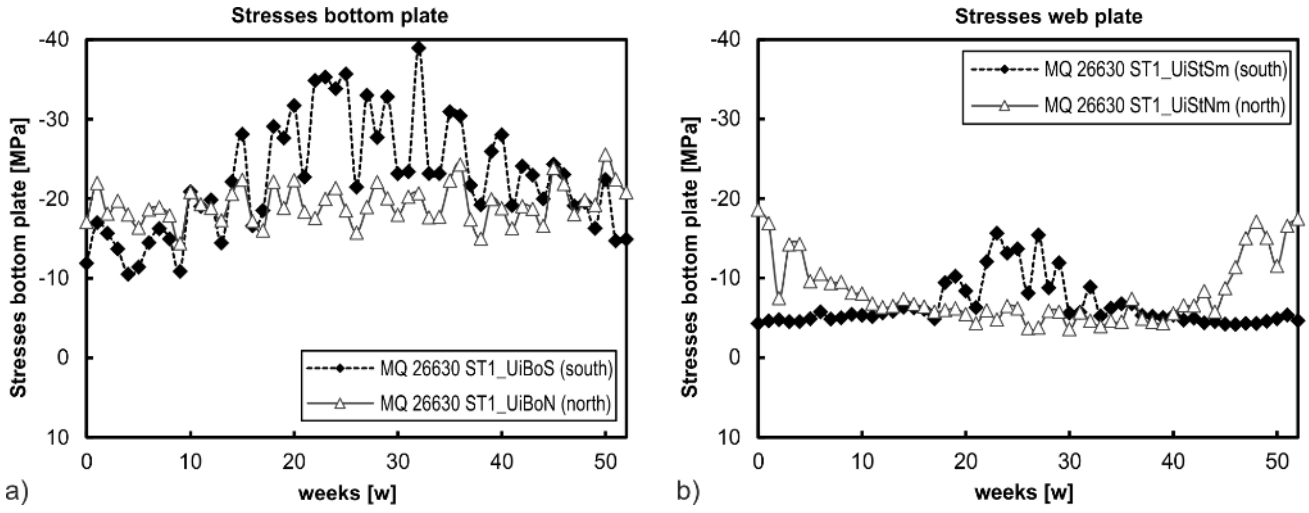

Figure 9. Weekly minima of the measuring points a) 26330 ST1_UiBoS (south side); b) 26330 ST1_UiBoN (north side) (source: WTM Engineers)

DOI: 10.3217/978-3-99161-057-1-017

south side (Fig. 9a) show a clear influence of the seasonal temperature profile compared to the same measuring point on the north side. Analyses of the different types of actions have shown that influences from direct sunlight are much more pronounced at this measuring point, which explains the stronger basic variance. In addition, there likely is a local temperature-related constraint that does not exist in this form on the north side. Similar effects are visible for the evaluation of the web stresses, whereby these are due to the influence of direct solar radiation (Fig. 9b). A more detailed investigation was carried out, which, however, is not the subject of this paper.

The distribution of the weekly extreme values of the two measuring points in the relevant measuring cross-section 26630 is shown in Fig. 10. The parameters of the extreme value distribution (type I) m_x (expected value) and σ_x (standard deviation) as well as the minimum compressive stress $\sigma_{s,min}$ recorded at the measuring point during the measuring period are each shown in the diagram. It can be seen that the Gumbel distribution represents a very good approximation of the actual distribution of the weekly extreme values at the measuring points investigated.

However, it is also clear that the distribution functions differ significantly with regard to the standard deviations. The critical stresses occur at the measuring point MQ 26630 ST1_UiBoS (Fig. 10a)) on the south side of the superstructure. The parameters of the distribution functions determined for the individual measuring points are the basis for the design stresses determined in the following.

4.2 Determination of the design values

Based on the weekly extreme values recorded during the measurement period and presented in the previous section, the design values of the action were determined with an extreme value distribution of type I according to the calculation steps explained in Section 3. Table 1 summarizes the target reliabilities β_t and $\beta_{E,t}$, the weighting factors α_E, characteristic values of the actions E_k and the design values E_d for different reference periods. The partial safety factors γ_Q result from the ratio of the design value E_d to the characteristic action E_k.

Table 1. Comparison of target reliability and characteristic expected values for different reference periods

Reference period t	1 year	50 years	100 years	200 years	1000 years
Target reliability β_t	4,68	3,80	3,62	3,44	2,98
Target reliability $\beta_{E,t}$	-3,78	-2,66	-2,42	-2,16	-1,44
Weighting factor $\alpha_E = \beta_{E,t} / \beta_t$	-0,81	-0,70	-0,67	-0,63	-0,48
Expected value $E_{k,t} = u(t)$ [MPa]	-41,27	-63,18	-67,05	-70,92	-79,91
Design value E_d	-94,2				
Partial safety factor $\gamma_Q = E_d/E_k$	2,28	1,49	1,40	1,33	1,18

The calculation of the design value of the stress is carried out below as an example for a reference period of 200 years. The parameters *a* and the model value *u* result in

$$a = \pi/(7.182 \cdot \sqrt{6}) = 0.179$$

and

$$u = 22.47 + 0.577216/0.179 = 19.25 \text{ MPa}$$

for the weekly extreme value distribution (initial values cf. Fig. 10a). The fractile value for determining the characteristic value E_k for a reference period of 200 years is

$$q = 1/(52 \cdot 200) = 9.615\text{E-}5.$$

The characteristic expected value is therefore

$$E_{k,200} = 19.25+1/0.179 \cdot LN[\ LN\ (1-9.615\text{E-}5)] = 70.92\text{MPa}.$$

The fractile value of the target reliability for the ULS for a reference period of 200 years is

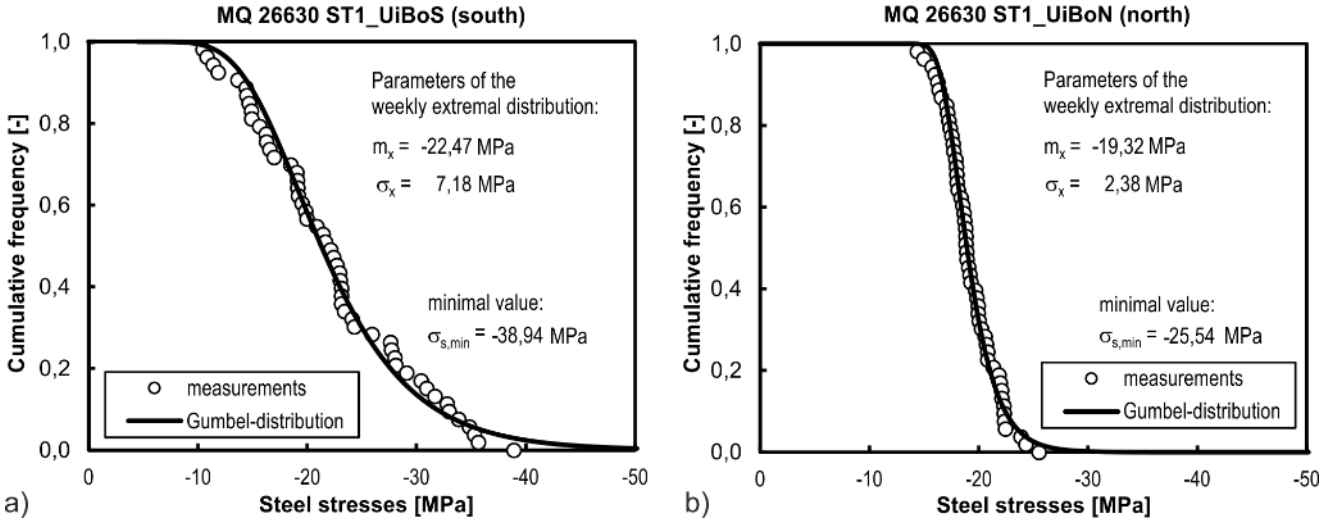

Figure 10. Distribution of the weekly extreme values in the base plate of measurement cross-section 26630 for a) the south side; b) the north side (source: WTM Engineers)

DOI: 10.3217/978-3-99161-057-1-017

$P_f = \Phi(\beta_{E,200}) = 1\text{-}[1\text{-}\Phi(\text{-}0.7\cdot 3.8)]^{200/50} = 1.539E\text{-}2$

(here the reliability index for a reference period of 50 years is the starting point). This corresponds to a safety index of

$\beta_{E,200} = \Phi^{-1}(1{,}539E\text{-}2) = -2.16.$

The design value thus results in

$E_d = -70.92+1\text{-}0.179\cdot \text{LN}[\text{LN}(1\text{-}1{,}539E\text{-}2)] = 94.2$ MPa.

Based on this evaluation, it can be determined that the safety against buckling can also be provided for the safety level applicable to new structures with a significant safety margin. The ratio of permissible compressive stress to design compressive stress ($\eta = \sigma_{Q,Rd} / \sigma_{Q,Ed}$) is $\eta = 113/94.2 = 1.20$.

4.3 Additional stress due to lifting of the distance requirement

The calculations to date reflect the state of traffic under the distance requirement in force during the measurement period. However, one aim of the permanent monitoring was to lift the current distance requirement in the event that sufficient safety reserves arise with regard to the buckling proof. One question to be clarified is the extent to which the stresses are likely to increase as a result of the removal of the distance requirement. According to Table A1-3 of the NRR [17], the traffic compensation measures of a truck overtaking ban and a truck distance requirement of 50 m correspond to a reduction of the target load level from LM1 to BK60.

In simplified terms, the load can increase from load model BK60 to LM1 if the spacing requirement is lifted. A comparison of the UDL loads distributed over a large area of the load models BK60 and LM1 results in a potential increase of $q_{LM1}/q_{BK60} = 1.18$ if the traffic mix is largely maintained when the distance requirement is lifted.

According to the recalculation of the Köhlbrand Bridge [15], the share of traffic loads in the variable loads is approx. 50 %. This means that an increase in the traffic load by 18 % results in an increase in the variable loads by a total of around 9 %. Even if the distance requirement is lifted, the buckling check is not expected to fall below the safety requirements for new structures. In any case, permanent monitoring would be continued if the distance requirement is lifted in order to be able to assess the actual effects on buckling safety.

4.4 Dynamic monitoring of reliability

To enable dynamic monitoring of reliability as a condition indicator, the existing safety index can be calculated for a reference period of 50 years to assess the buckling safety with

$$\beta_{E,50,prov} = \Phi^{-1}(F(\sigma_{Q,Rd})) = \Phi^{-1}(1\text{-}\exp[\text{-}\exp(0{,}179\cdot(\text{-}113 + 63{,}18))]) = \text{-}3{,}64$$

(with $\sigma_{Q,Rd} = 113$ MPa).

In continuous long-term monitoring, the existing safety index $\beta_{E,50,prov}$ can be updated weekly in this way. This is shown as an example in Fig. 11. From the 25th week of long-term monitoring, the database for calculating the existing reliability $\beta_{E,50,\,prov}$ is expanded and updated by one value every week. In this way, $\beta_{E,50,\,prov}$ approaches the final value of -3.64 after one year of monitoring. If the distance requirement is lifted, the effects on buckling safety can be assessed immediately after a few weeks using this diagram. The advantage of this reliability-based parameter is that it reflects the cumulative load history and exceptional load events can be directly classified here. In addition, lower reliability requirements can be defined as threshold values for existing structures with a short remaining service life. The advantage of this parameter is also that, unlike a degree of utilization, its threshold values are independent of the kind of verification to be performed (and therefore do not have to be scaled) and the procedure shown here is therefore transferable to other types of verification.

4.5 Integration into the digital twin of the Köhlbrand Bridge

The condition indicator described above was used as part of a higher-level project to develop a digital twin of the Köhlbrand Bridge [19] and integrated directly into the system. The system is based on a BIM model of the current bridge and the ramp structures and combines the available information from structure books, the German digital structures database (SIB), information from structure diagnostics and the structure monitoring within one system. Instead of operating separate data silos, all available key information on the condition of the structure is combined in one system. A major advantage is that it is much easier to recognize correlations between different sources of information. For example, information on structural damage is displayed directly in the 3D model (Fig. 12).

The taxonomy of the BIM model is based on the component groups according to the German taxonomy code ASB-ING. For the “Strombrücke” substructure of the Köhlbrand Bridge, a condition indicator was developed for each component group, which summarizes all available information on the component group into a condition group. A procedure was developed to combine the condition scores from the structural inspections with the information from structural monitoring to form a condition score [28]. Fig. 13a shows the condition indicator “superstructure” (steel box girder). The overall condition of the

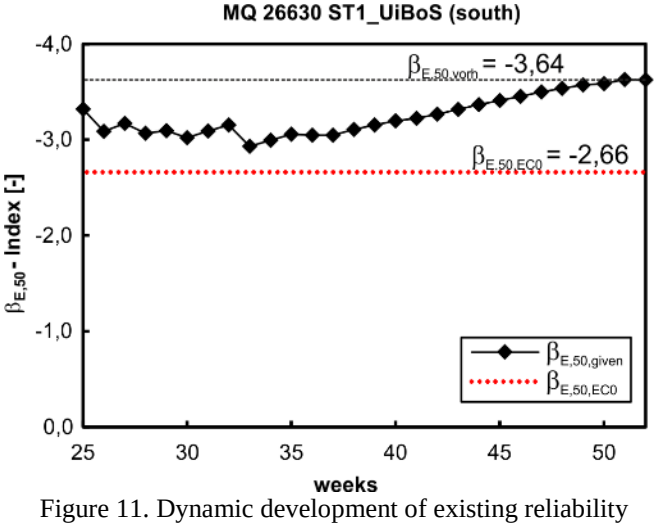

Figure 11. Dynamic development of existing reliability from long-term monitoring (source: WTM Engineers)

DOI: 10.3217/978-3-99161-057-1-017

Figure 12. Visualization of structural damage information (source: MKP GmbH)

superstructure results from the PCI (Partial Condition Indicator) of the structural inspection and the PCI of the measurement-based calculations. With the PCIs "buckling safety" and "fatigue safety of transverse frame", the CI includes the monitoring of two potential damage scenarios that were classified as critical for the structure based on sensitivity analyses.

The buckling safety is assessed by the previously described probabilistic evaluation of the strains measured at the areas at risk of buckling (Fig. 13b). The calculation of the existing safety index for buckling failure on the basis of structural measurements is explained in Section 4. The reliability index (here β_E-index, related to the action side) is permanently determined from the existing measurement data, which in turn is converted into a condition rating as explained in [28],[29]. In the visualization, the changes in the condition scores are shown in order to illustrate the effect of the damage scenario under consideration on the overall structure. In addition, a time diagram with the development of the reliability index over time is shown to illustrate the development of the condition over time and, if necessary, for an initial plausibility check.

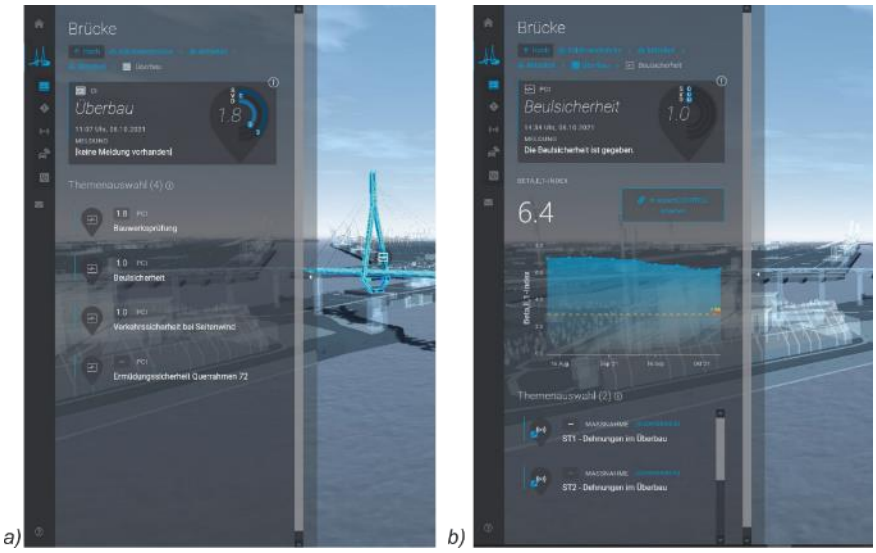

Figure 13. Visualizations in the Condition Control smartBRIDGE Hamburg of the a) CI "Superstructure" of the Köhlbrand Bridge with the associated PCIs; b) Detailed view of the PCI "Buckling safety" (source: MKP GmbH)

5 SUMMARY AND OUTLOOK

In this paper, long-term buckling monitoring data from a twelve-month period from July 2019 to June 2020 was evaluated to derive a reliability-based condition indicator for assessing the risk of buckling of the Köhlbrand Bridge superstructure. The aim was to use probabilistic methods to determine whether there is a risk of buckling for the superstructure in the current load situation with a distance requirement in place and whether there are sufficient load reserves to lift the distance requirement.

The statistical evaluation of the weekly extreme values showed that the critical stress values occur on the south side in the pylon area of the superstructure. As expected, the distribution of the measured values could be approximated very well by a type I extreme value distribution. Based on the distribution function, the design values of the variable actions were determined and compared with the structural resistances. This data was used to derive a time-variable reliability index as a condition indicator, which places exceptional load events in the context of the load history and whose threshold values can be defined independently of the verification to be performed. In this example, there were sufficient reserves to lift the distance requirement. Continuous monitoring will nevertheless be continued, also in order to be able to assess the actual effects on safety against buckling if the distance requirement is lifted. In a further step, the condition indicator described in this article was implemented with other condition indicators as part of the smartBRIDGE Hamburg project in a digital twin of the Köhlbrand Bridge. By combining and aggregating all available information on the condition of the structure into a condition score, operators and structural engineers can immediately identify any need for action on the structure.

DOI: 10.3217/978-3-99161-057-1-017

REFERENCES

[1] BMVBS (2011) Richtlinie zur Nachrechnung von Straßenbrücken im Bestand (Nachrechnungsrichtlinie). Ausgabe 05/2011
[2] Böning S. (2013) Entwicklung einer geschlossenen Vorgehensweise zur Ermittlung von Beanspruchungen von Brückenbauwerken infolge Straßenverkehr. Dissertation Bauhaus Universität Weimar, Düren: Shaker Verlag
[3] Nowak, M.; Fischer, O. (2017) Objektspezifische Verkehrslastansätze für Straßenbrücken in: Beton- und Stahlbetonbau 112, H. 12, S. 804–814
[4] Geißler, K.; Steffens, N.; Stein, R. (2019) Grundlagen der sicherheitsäquivalenten Bewertung von Brücken mit Bauwerksmonitoring in: Stahlbau 88, H. 4, S. 338–353
[5] Frangopol, D. M.; Strauss, A.; Kim, S. (2008) Use of monitoring extreme data for the performance prediction of structures: General approach in: Engineering Structrues 30, S. 3644-3653
[6] Strauss, A.; Frangopol, D. M.; Kim, S. (2008) Use of monitoring extreme data for the performance prediction of structures: Bayesian Updating in: Engineering Structrues 30, S. 3654-3666
[7] Liu, M.; Frangopol, D. M.; Kim, S. (2009) Bridge Safety Evaluation Based on Monitored Live Load Effects in: Journal of Bridge Engineering 14, S. 257–269
[8] Frangopol, D. M.; Strauss, A.; Kim, S. (2008) Bridge Reliability Assessment Based on Monitoring in: Journal of Bridge Engineering 13, S. 258–270
[9] Treacy, M. A.; Brühwiler, E.; Caprani, C. C. (2013) Monitoring of traffic action local effects in highway bridge deck slabs and the influence of measurement duration on extreme value estimates in: Structure and Infrastructure Engineering 10, Iss. 12, S. 1555-1572
[10] Anderegg, P.; Brönnimann, R.; Meier, U. (2018) Referenzmessdaten beim Langzeitmonitoring von Infrastrukturen in: Bautechnik 95, H. 7, S. 494–498
[11] Frangopol, D. M.; Saydam, D. (2014) Structural Performance Indicators for Bridges in: Bridge Engineering Handbook, 2nd Edition, S. 185–205, CRC Press
[12] Ang, A. H.-S.; Tang, W. H. (1984) Probability Concepts in Engineering Planning and Design - Volume II. Singapore: John Wiley & Sons
[13] Boué, P.; Höhne, K.-J. (1975) Der Stromüberbau der Köhlbrandbrücke in: Stahlbau 44, H. 6, S. 161–174 & H. 7, S. 203–211
[14] LAP AG (2015) Köhlbrandbrücke Strombrücke (Los 1) - Nachrechnung Statische Berechnung (Stufe 1). Leonhardt, Andrä und Partner VBI AG, 25. Juni 2015
[15] LAP AG (2016) Köhlbrandbrücke Strombrücke (Los) - Nachrechnung Stufe 3 Statische Berechnung. Leonhardt, Andrä und Partner VBI AG, 30. Juni 2016
[16] DIN-Fachbericht 103 (2009) Stahlbrücken. Ausgabe 03/2009
[17] BMVI (2015) Richtlinie zur Nachrechnung von Straßenbrücken im Bestand (Nachrechnungsrichtlinie) - 1. Ergänzung. Ausgabe 04/2015
[18] DIN 1072 (1967) Straßen- und Wegbrücken, Lastannahmen. Ausgabe 11/1967
[19] Grabe, M.; Ullerich, C.; Wenner, M.; Herbrand, M. (2020) smartBridge Hamburg – prototypische Pilotierung eines digitalen Zwillings in: Bautechnik 97, H. 2, S. 118–125
[20] Matz, F. (2020) Messtechnisch gestützte Überwachung von Brückentragwerken am Beispiel der Hamburger Köhlbrandbrücke. Diplomarbeit, TU Dresden
[21] DIN EN 1990 (2010) Grundlagen der Tragwerksplanung Ausgabe 12/2010 + A1:08/2012, Berlin: Beuth Verlag
[22] Steffens, N.; Degenhardt, K.; K. Geißler, K. (2019) Modifiziertes Ziellastniveau bei Straßenbrücken durch Bauwerksmonitoring in: Schriftenreihe Konstruktiver Ingenieurbau Dresden, Heft 48 2019
[23] Spaethe, G. (1992) Die Sicherheit tragender Baukonstruktionen. 2. Auflage, Wien: Springer-Verlag
[24] Steffens, N. (2019) Sicherheitsäquivalente Bewertung von Brücken durch Bauwerksmonitoring. Dissertation TU Berlin, Düren: Shaker Verlag
[25] DIN EN 1991-2 Einwirkungen auf Tragwerke – Verkehrslasten auf Brücken Ausgabe 12/2010, Berlin: Beuth Verlag
[26] Freundt, U.; Vogt, R.; Böning, S.; Michael, D. (2014) Einsatz von Monitoringsystemen zur Bewertung des Schädigungszustands von Brückenbauwerken. Forschungsbericht, BASt Heft B 106
[27] DIN 1055-100 (2001) Einwirkungen auf Tragwerke - Teil 100: Grundlagen der Tragwerksplanung, Sicherheitskonzept und Bemessungsregeln. Ausgabe 03/2001, Berlin: Beuth Verlag
[28] Herbrand, M. et al.: Aggregation von Zustandsindikatoren aus Inspektions- und Monitoringdaten im Brückenbau in: Bautechnik 99, H. 2, S. 95–103
[29] Herbrand, M. et al.: Beurteilung der Bauwerkszuverlässigkeit durch Bauwerksmonitoring in: Bautechnik 98, H. 2, S. 93–104